Journal of Sound and Vibration (1998) **215**(1), 143–165
Article No. sv982556

VIBRATION OF A T-TYPE CURVED FRAME DUE TO A MOVING FORCE

R. T. WANG

Department of Engineering Science, National Cheng Kung University
Taiwan, Republic of China

(*Received* 27 *September* 1997, *and in final form* 10 *March* 1998)

This work presents the formulation of governing equations for a curved frame. An analytic method is also presented to examine the vibration of the curved frame. The orthogonality of any two distinct sets of mode shape functions of the frame is also derived. The forced vibration of the frame owing to a moving concentrated force is examined. The strain energy characteristics of the frame induced by the moving force are investigated as well.

1. INTRODUCTION

An elevated guideway can be simulated as a frame structure. Beams and columns of the frame are normally organized in a straight type. Owing to the restriction of space and environment, beams of the frame are sometimes arranged into a curved type. The geometry of a curved frame completely differs from that of a straight frame. The equations of motion of a straight frame structure can be easily described via the Bernoulli–Euler beam theory or the Timoshenko beam theory under the conditions of displacements continuity and of force balance at the junction of one column with two adjacent beams. However, the equations of motion for a curved frame have never been set. The initial curvature of a curved frame causes a torque to exist in the structure. The torsional vibration of a curved frame owing to a moving vehicle causes the passengers to feel uncomfortable. The initial curvature of a curved frame and the velocity of loads are, therefore, two important factors of governing the responses of the structure caused by the moving loads. The responses of a straight frame due to an external load can be obtained either by the method of finite element method [1] or by the method of modal analysis [2]. However, the method of modal analysis for examining the responses of a curved frame has never been found till now.

The out-of-plane deflection of a curved beam due to a static load has been examined for over two decades [3–5]. The vehicles traversing on the structure are more rapid than before. The responses of a structure due to a moving load in general exceed those of the structure by the load in a static situation. Experimental results indicate that the dynamic impact on the frame owing to moving loads should be included for designing the structure. By neglecting the warping effect of a compact solid, the free vibration for out-of-plane motion of a curved beam has also been investigated for the past two decades [6–8]. However, the study for the forced vibration of a curved beam has never been mentioned. Wang and Sang [9] set the displacement fields to derive the equations for out-of-plane motion of a multi-span curved beam. Furthermore, they presented an analytical method

0022–460X/98/310143 + 23 $30.00/0

to examine the forced vibration of the multi-span curved beam due to moving loads. The axial inertia is normally neglected in studying the vibration of a curved beam. A T-type straight frame is a special type of the curved frame. The displacement fields of a T-type straight frame contain a bending slope, a transverse displacement and a longitudinal displacement. Further, the effects of longitudinal inertia, transverse inertia, rotatory inertia, longitudinal force, transverse shear force and bending moment of each branch of the T-type straight frame should be included simultaneously for examining the vibration of the structure. However, the geometry of a T-type curved frame causes the displacement fields of the structure to be more complex than those of a T-type straight frame. Two bending slopes, a twist angle, two transverse displacements and a longitudinal displacement are needed to describe the displacement fields of a T-type curved frame. Furthermore, the corresponding bending moments, torque, transverse shear forces and axial force should be included simultaneously for deriving the equations of motion of the frame.

This study presents the displacement fields of a T-type curved frame. The frame has a continuous curved beam resting on a column. The frame is considered to be compact, homogeneous and isotropic with Young's modulus E, shear modulus G, Poisson's ratio μ and mass density ρ. The continuous curved beam has a rectangular cross-section. The column has a circular cross-section. The strains are derived to obtain the stress resultants and stress-couple resultants in the frame. Via the Hamilton's principle, the equations of motion of the entire structure are set. An analytical method is presented to obtain the modal frequencies and their corresponding sets of mode shape functions of the frame. The orthogonality of any two distinct sets of mode shape functions is derived to show the feasibility of the method of modal analysis. The forced vibration of the curved frame due to a moving force is then examined by the method. Usually, the damage of the structure is governed by its strain energy density. Therefore, the strain energy density and the strain energy of the frame induced by the moving force are investigated to understand the general feature of the responses of the structure. The effects of the velocity of the force and the column height of the frame on the characteristics of strain energy are also examined.

2. GOVERNING EQUATIONS

A distributed load $f(\theta, t)$ acting on a frame is depicted in Figure 1. All ends of the frame are fixed. The radius of the curved beam is R. The angle measured from one fixed end to the junction of two adjacent beams and the column is α. The column has the height h.

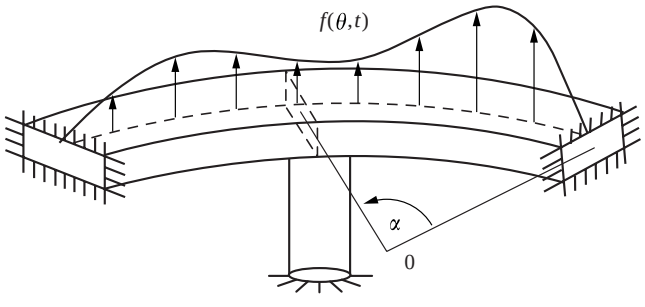

Figure 1. A distributed load $f(\theta, t)$ on the curved frame.

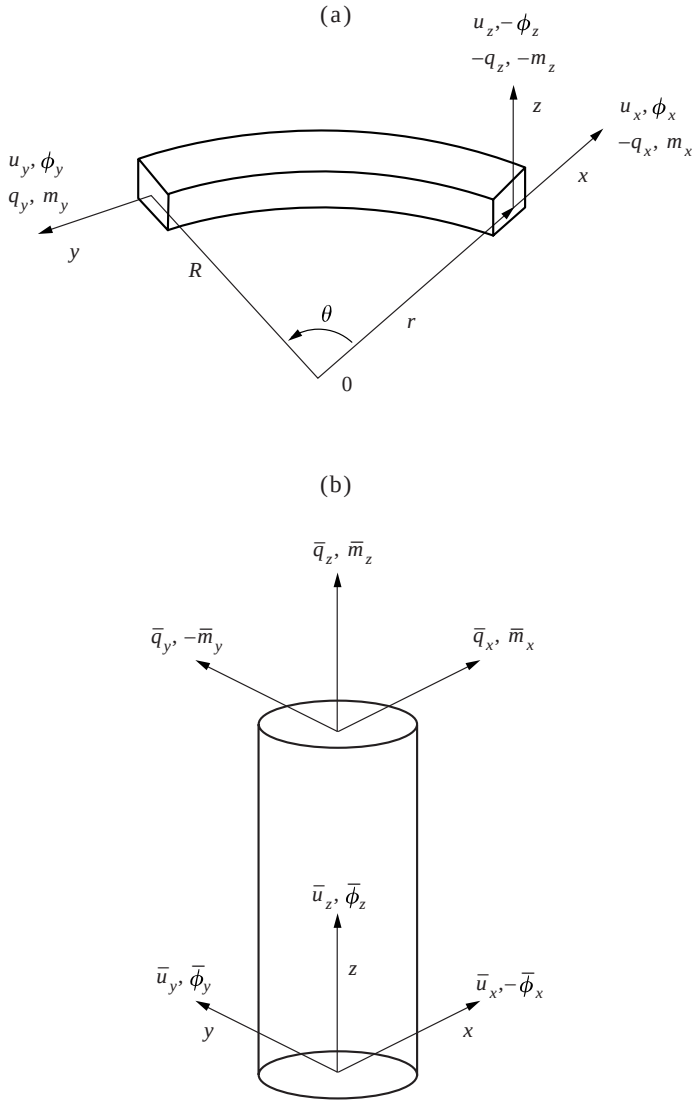

Figure 2. Displacements, stress resultants and stress couple resultants for (a) a typical curved beam and (b) the column of the frame.

2.1. EQUATIONS OF MOTION OF THE CURVED BEAM

The Cartesian co-ordinates x, y and z system and the cylindrical co-ordinates r, θ and z system are depicted in Figure 2(a). The x and z axes coincide with the principal centroidal axes of the beam, while the y-axis is tangent to the curved axis of the beam. The co-ordinates r, θ and z are taken at the centre of the beam. The beam has width a, thickness b, uniform cross-sectional area A, polar moment J about the y-axis, shear coefficient κ_1, second moments of area I_x and I_z about the x-axis and z-axis, respectively. Further, the width a is assumed to be less than the radius R of the curved beam. The displacement components along these principal axes are denoted as u_x, u_y and u_z, respectively. Furthermore, ϕ_x, ϕ_y and ϕ_z are the respective rotation angles of the cross-section along these principal axes.

By neglecting the warping effect of the cross-section, the displacement fields of the curved beam along these principal axes in the Cartesian co-ordinates are expressed as

$$u_x^*(x, y, z, t) = u_x(y, t) + z\phi_y(y, t),$$

$$u_y^*(x, y, z, t) = u_y(y, t) - z\phi_x(y, t) - x\phi_z(y, t),$$

$$u_z^*(x, y, z, t) = u_z(y, t) - x\phi_y(y, t), \tag{1a}$$

or in the cylindrical co-ordinates as

$$u_r^* = u_x^*, \quad u_\theta^* = u_y^*, \quad u_z^* = u_z^*, \quad \phi_\theta = \phi_y, \quad u_\theta = u_y, \tag{1b}$$

The strain components in the cylindrical co-ordinates are

$$\varepsilon_{rr} = \frac{\partial u_r^*}{\partial r}, \qquad \varepsilon_{\theta\theta} = \frac{1}{r}\frac{\partial u_\theta^*}{\partial \theta} + \frac{u_r^*}{r}, \qquad \varepsilon_{zz} = \frac{\partial u_z^*}{\partial z},$$

$$\gamma_{r\theta} = \frac{\partial u_\theta^*}{\partial r} + \frac{1}{r}\frac{\partial u_r^*}{\partial \theta} - \frac{u_\theta^*}{r}, \qquad \gamma_{rz} = \frac{\partial u_r^*}{\partial z} + \frac{\partial u_z^*}{\partial r}, \qquad \gamma_{\theta z} = \frac{\partial u_\theta^*}{\partial z} + \frac{1}{r}\frac{\partial u_z^*}{\partial \theta}, \tag{2}$$

By using the geometric relations $y = R\theta$ and $r = R + x$, the strains in the Cartesian co-ordinates are obtained as

$$\varepsilon_{xx} = 0, \quad \varepsilon_{zz} = 0, \quad \gamma_{zx} = 0, \quad \varepsilon_{yy} = \frac{R}{r}\left[\frac{\partial u_y}{\partial y} + \frac{u_x}{R} + z\left(\frac{\phi_y}{R} - \frac{\partial \phi_x}{\partial y}\right) - x\frac{\partial \phi_z}{\partial y}\right],$$

$$\gamma_{xy} = \frac{R}{r}\left[\left(-\phi_z + \frac{\partial u_x}{\partial y} - \frac{u_y}{R}\right) + z\left(\frac{\partial \phi_y}{\partial y} + \frac{\phi_x}{R}\right)\right], \qquad \gamma_{yz} = \frac{R}{r}\left(-\frac{r\phi_x}{R} + \frac{\partial u_z}{\partial y} - x\frac{\partial \phi_y}{\partial y}\right). \tag{3}$$

Employing the relation

$$\frac{R}{r} = \frac{R}{R + x} = \frac{1}{1 + \dfrac{x}{R}} = 1 - \left(\frac{x}{R}\right) + \left(\frac{x}{R}\right)^2 + \cdots$$

into equation (3) and neglecting the terms $O(x/R)$ yields

$$\varepsilon_{xx} = 0, \quad \varepsilon_{zz} = 0, \quad \gamma_{zx} = 0, \qquad \varepsilon_{yy} = \frac{\partial u_y}{\partial y} + \frac{u_x}{R} + z\left(\frac{\phi_y}{R} - \frac{\partial \phi_x}{\partial y}\right) - x\frac{\partial \phi_z}{\partial y},$$

$$\gamma_{xy} = -\phi_z + \frac{\partial u_x}{\partial y} - \frac{u_y}{R} + z\left(\frac{\partial \phi_y}{\partial y} + \frac{\phi_x}{R}\right), \qquad \gamma_{xy} = -\phi_x + \frac{\partial u_z}{\partial y} - x\left(\frac{\partial \phi_y}{\partial y} + \frac{\phi_x}{R}\right). \tag{4}$$

The stress resultants q_x, $q_y(=q_\theta)$ and q_z, and stress-couple resultants m_x, $m_y(=m_\theta)$ and m_z of the curved beam about these principal axes are (Figure 2(a))

$$q_x = \kappa_1 GA\left(\frac{1}{R}\frac{\partial u_x}{\partial\theta} - \phi_z - \frac{u_\theta}{R}\right), \qquad q_\theta = q_y = EA\left(\frac{1}{R}\frac{\partial u_\theta}{\partial\theta} + \frac{u_x}{R}\right), \tag{5a, b}$$

$$q_z = \kappa_1 GA\left(\frac{1}{R}\frac{\partial u_z}{\partial\theta} - \phi_x\right), \qquad m_x = \frac{EI_x}{R}\left(\phi_\theta - \frac{\partial\phi_x}{\partial\theta}\right), \tag{5c, d}$$

$$m_\theta = m_y = \frac{C}{R}\left(\phi_x + \frac{\partial\phi_\theta}{\partial\theta}\right), \qquad m_z = -\frac{EI_z}{R}\frac{\partial\phi_z}{\partial\theta}, \tag{5e, f}$$

where $C\ (=\kappa_3 Gab^3)$ denotes the torsional rigidity and κ_3 represents the torsion coefficient [10].

The strain energy $S_b(t)$ of the curved beam is

$$S_b(t) = \frac{1}{2}\int_0^{2\alpha}\left\{\frac{q_\theta^2}{EA} + \frac{q_x^2}{\kappa_1 GA} + \frac{q_z^2}{\kappa_1 GA} + \frac{m_x^2}{EI_x} + \frac{m_\theta^2}{C} + \frac{m_z^2}{EI_z}\right\}R\,\mathrm{d}\theta. \tag{6}$$

The kinetic energy $K(t)$ of the curved beam is

$$K(t) = \frac{1}{2}\int_0^{2\alpha}\left\{\rho A\left[\left(\frac{\partial u_x}{\partial t}\right)^2 + \left(\frac{\partial u_\theta}{\partial t}\right)^2 + \left(\frac{\partial u_z}{\partial t}\right)^2 + \rho J\left(\frac{\partial\phi_\theta}{\partial t}\right)^2\right]\right.$$

$$\left. + \rho I_x\left(\frac{\partial\phi_x}{\partial t}\right)^2 + \rho I_z\left(\frac{\partial\phi_z}{\partial t}\right)^2\right\}R\,\mathrm{d}\theta. \tag{7}$$

The energy E_f put into this frame by the distributed load $f(\theta, t)$ is

$$E_f(t) = \int_0^{2\alpha} f(\theta, t)u_z R\,\mathrm{d}\theta. \tag{8}$$

Performing Hamilton's principle yields the following six equations of motion of the curved beam

$$\frac{q_\theta}{R} - \frac{1}{R}\frac{\partial q_x}{\partial\theta} + \rho A\frac{\partial^2 u_x}{\partial t^2} = 0, \qquad -\frac{q_x}{R} - \frac{1}{R}\frac{\partial q_\theta}{\partial\theta} + \rho A\frac{\partial^2 u_\theta}{\partial t^2} = 0, \tag{9a, b}$$

$$-\frac{1}{R}\frac{\partial q_z}{\partial\theta} + \rho A\frac{\partial^2 u_z}{\partial t^2} = f(\theta, t), \qquad -q_z + \frac{1}{R}\frac{\partial m_x}{\partial\theta} + \frac{m_\theta}{R} + \rho I_x\frac{\partial^2\phi_x}{\partial t^2} = 0, \tag{9c, d}$$

$$-\frac{1}{R}\frac{\partial m_\theta}{\partial\theta} + \frac{m_x}{R} + \rho J\frac{\partial^2\phi_\theta}{\partial t^2} = 0, \qquad -q_x + \frac{1}{R}\frac{\partial m_z}{\partial\theta} + \rho I_z\frac{\partial^2\phi_z}{\partial t^2} = 0. \tag{9e, f}$$

The displacements, rotations, stress resultants and stress-couple resultants of the ith span of the entire beam are expressed as

$$(u_{xi}\ u_{\theta i}\ u_{zi}\ \phi_{xi}\ \phi_{\theta i}\ \phi_{zi})(\theta, t) = (u_x\ u_\theta\ u_z\ \phi_x\ \phi_\theta\ \phi_z)[\theta + (i-1)\alpha, t], \tag{10a}$$

$$(q_{xi}\ q_{\theta i}\ q_{zi}\ m_{xi}\ m_{\theta i}\ m_{zi})(\theta, t) = (q_x\ q_\theta\ q_z\ m_x\ m_\theta\ m_z)[\theta + (i-1)\alpha, t]. \tag{10b}$$

Furthermore, the sign conventions for displacements, rotations, stress resultants and stress-couple resultants at two ends of the ith span of the entire beam are denoted as

$$\{d_r\}_i(t) = \{u_{xi}\ u_{\theta i}\ u_{zi}\ \phi_{xi}\ \phi_{\theta i}\ -\phi_{zi}\}^T(0, t), \tag{11a}$$

$$\{f_r\}_i(t) = \{-q_{xi}\ -q_{\theta i}\ -q_{zi}\ m_{xi}\ -m_{\theta i}\ -m_{zi}\}^T(0, t), \tag{11b}$$

$$\{d_l\}_i(t) = \{u_{xi}\ u_{\theta i}\ u_{zi}\ \phi_{xi}\ \phi_{\theta i}\ -\phi_{zi}\}^T(\alpha, t), \tag{11c}$$

$$\{f_l\}_i(t) = \{q_{xi}\ q_{\theta i}\ q_{zi}\ -m_{xi}\ m_{\theta i}\ m_{zi}\}^T(\alpha, t). \tag{11d}$$

2.2. EQUATIONS OF MOTION OF COLUMN

The Cartesian co-ordinates x, y and z system of the cylindrical column are depicted in Figure 2(b). The x and y axes coincide with the principal centroidal axes of the column, while the z-axis denotes the longitudinal axis of the column. The column has a uniform cross-sectional area A^*, polar moment J^* around the z-axis, shear coefficient κ_2, second moment of area I^* around the x-axis (or y-axis). u_x, u_y, and u_z are the respective displacement components along these principal axes. Furthermore, ϕ_x, ϕ_y, and ϕ_z are the rotation angles of the cross-section along the principal axes, respectively. The displacement fields of the column along these principal axes in the Cartesian co-ordinates are

$$\overline{u_x}^*(x, y, z, t) = \overline{u_x}(z, t) - y\overline{\phi_z}(z, t), \qquad \overline{u_y}^*(x, y, z, t) = \overline{u_y}(z, t) + x\overline{\phi_z}(z, t),$$
$$\overline{u_z}^*(x, y, z, t) = \overline{u_z}(z, t) - x\overline{\phi_y}(z, t) - y\overline{\phi_x}(z, t). \tag{12a, b, c}$$

The stress resultants $\overline{q_x}$, $\overline{q_y}$ and $\overline{q_z}$, and stress-couple resultants $\overline{m_x}$, $\overline{m_y}$ and $\overline{m_z}$ of the beam about these principal axes are (Figure 2(b))

$$\overline{q_x} = \kappa_2 GA^*\left(\frac{\partial\overline{u_x}}{\partial z} - \overline{\phi_y}\right), \qquad \overline{q_y} = \kappa_2 GA^*\left(\frac{\partial\overline{u_y}}{\partial z} - \overline{\phi_x}\right), \qquad \overline{q_z} = EA^*\frac{\partial\overline{u_z}}{\partial z}, \tag{13a, b, c}$$

$$\overline{m_x} = -EI^*\frac{\partial\overline{\phi_x}}{\partial z}, \qquad \overline{m_y} = -EI^*\frac{\partial\overline{\phi_y}}{\partial z}, \qquad \overline{m_z} = GJ^*\frac{\partial\overline{\phi_z}}{\partial z}. \tag{13d, e, f}$$

Similarly, the following six equations of motion of this column are

$$-\frac{\partial\overline{q_x}}{\partial z} + \rho A^*\frac{\partial^2\overline{u_x}}{\partial t^2} = 0, \qquad -\frac{\partial\overline{q_y}}{\partial z} + \rho A^*\frac{\partial^2\overline{u_y}}{\partial t^2} = 0, \tag{14a, b}$$

$$-\frac{\partial\overline{q_z}}{\partial z} + \rho A^*\frac{\partial^2\overline{u_z}}{\partial t^2} = 0, \qquad -\overline{q_y} + \frac{\partial\overline{m_x}}{\partial z} + \rho I^*\frac{\partial^2\overline{\phi_x}}{\partial t^2} = 0, \tag{14c, d}$$

$$-\overline{q_x} + \frac{\partial\overline{m_y}}{\partial z} + \rho I^*\frac{\partial^2\overline{\phi_y}}{\partial t^2} = 0, \qquad -\frac{\partial\overline{m_z}}{\partial z} + \rho J^*\frac{\partial^2\overline{\phi_z}}{\partial t^2} = 0. \tag{14e, f}$$

The sign conventions for displacements, rotations, stress resultants and the stress-couple resultants at the top end of the column are

$$\{\overline{d_l}\}(t) = \{\overline{u_x}\ \overline{u_y}\ \overline{u_z}\ -\overline{\phi_x}\ \overline{\phi_y}\ \overline{\phi_z}\}^T(h, t), \tag{15a}$$

$$\{\overline{f_l}\}(t) = \{\overline{q_x}\ \overline{q_y}\ \overline{q_z}\ \overline{m_x}\ -\overline{m_y}\ \overline{m_z}\}^T(h, t). \tag{15b}$$

2.3. BOUNDARY CONDITIONS

The boundary conditions at all fixed ends of the frame are

$$\{d_r\}_1 = \{d_l\}_2 = \{\overline{d_r}\} = \{0\ 0\ 0\ 0\ 0\ 0\}^T,$$
$$(\overline{u_x}, \overline{u_y}, \overline{u_z}, \overline{\phi_x}, \overline{\phi_y}, \overline{\phi_z})(0, t) = (0\ 0\ 0\ 0\ 0\ 0), \tag{16a, b}$$

in which subscript 1 (or 2) implies the first span (or the second span). The displacements continuity, forces balance and moments balance at the junction of two adjacent spans and the column are

$$\{d_l\}_1 = \{d_r\}_2 = \{\bar{d}_l\}, \qquad \{f_l\}_1 + \{f_r\}_2 + \{\bar{f}_l\} = \{0\ 0\ 0\ 0\ 0\ 0\}^T. \tag{17a, b}$$

3. MODAL FREQUENCIES

3.1. CURVED BEAM

To calculate the modal frequencies of the structure, the displacements, rotation angles and their corresponding stress resultants and stress-couple resultants of the ith span of curved beam are denoted as

$$\{u_{xi}\ u_{\theta i}\ u_{zi}\ \phi_{xi}\ \phi_{\theta i}\ \phi_{zi}\}(\theta, t) = \{U_{xi}\ U_{\theta i}\ U_{zi}\ \Phi_{xi}\ \Phi_{\theta i}\ \Phi_{zi}\}(\theta) \sin(\omega t), \tag{18a}$$

$$\{q_{xi}\ q_{\theta i}\ q_{zi}\ m_{xi}\ m_{\theta i}\ m_{zi}\}(\theta, t) = \{Q_{xi}\ Q_{\theta i}\ Q_{zi}\ M_{xi}\ M_{\theta i}\ M_{zi}\}(\theta) \sin(\omega t), \tag{18b}$$

where

$$Q_{xi} = \frac{\kappa_1 GA}{R}\left(\frac{\mathrm{d}U_{xi}}{\mathrm{d}\theta} - R\Phi_{zi} - U_{\theta i}\right), \qquad Q_{\theta i} = \frac{EA}{R}\left(\frac{\mathrm{d}U_{\theta i}}{\mathrm{d}\theta} + U_{xi}\right), \tag{19a, b}$$

$$Q_{zi} = \kappa_1 GA\left(\frac{1}{R}\frac{\mathrm{d}U_{zi}}{\mathrm{d}\theta} - \Phi_{xi}\right), \qquad M_{xi} = \frac{EI_x}{R}\left(\Phi_{\theta i} - \frac{\mathrm{d}\Phi_{xi}}{\mathrm{d}\theta}\right), \tag{19c, d}$$

$$M_{\theta i} = \frac{C}{R}\left(\Phi_{xi} + \frac{\mathrm{d}\Phi_{\theta i}}{\mathrm{d}\theta}\right), \qquad M_{zi} = -\frac{EI_z}{R}\frac{\mathrm{d}\Phi_{zi}}{\mathrm{d}\theta}, \tag{19e, f}$$

in which ω denotes the circular frequency. Further, the distributed load $f(\theta, t)$ is set at zero. Under these circumstances, equations (9a)–(9f) become

$$Q_{\theta i} - \frac{\mathrm{d}Q_{xi}}{\mathrm{d}\theta} = \rho AR\omega^2 U_{xi}, \qquad -Q_{xi} - \frac{\mathrm{d}Q_{\theta i}}{\mathrm{d}\theta} = \rho A\omega^2 R U_{\theta i}, \tag{20a, b}$$

$$-\frac{\mathrm{d}Q_{zi}}{\mathrm{d}\theta} = \rho A\omega^2 R U_{zi}, \qquad -RQ_{zi} + \frac{\mathrm{d}M_{xi}}{\mathrm{d}\theta} + M_{\theta i} = \rho I_x \omega^2 R\Phi_{xi}, \tag{20c, d}$$

$$-\frac{\mathrm{d}M_{\theta i}}{\mathrm{d}\theta} + M_{xi} = \rho J\omega^2 R\Phi_{\theta i}, \qquad -RQ_{xi} + \frac{\mathrm{d}M_{zi}}{\mathrm{d}\theta} = \rho I_z \omega^2 R\Phi_{zi}. \tag{20e, f}$$

Substituting Q_{xi} of equation (19a) and $Q_{\theta i}$ of equation (19b) into equation (20b) and solving Φ_{xi} in terms of U_{xi} and $U_{\theta i}$ yields the form

$$\Phi_{zi} = \frac{\kappa_1 G + E}{\kappa_1 GR}\frac{\mathrm{d}U_{xi}}{\mathrm{d}\theta} + \frac{1}{\kappa_1 GR}\left(\rho\omega^2 R^2 - \kappa_1 G + E\frac{\mathrm{d}^2}{\mathrm{d}\theta^2}\right)U_{\theta i}. \tag{21}$$

Substituting Q_{xi} of equation (19a) and $Q_{\theta i}$ of equation (19b) into equation (20a) and employing Φ_{zi} of equation (21) into the result yields

$$L_1(U_{xi}) + L_2(U_{\theta i}) = 0, \tag{22}$$

where

$$L_1(U_{xi}) = \left(\frac{\mathrm{d}^2}{\mathrm{d}\theta^2} + 1 - \frac{\rho\omega^2 R^2}{E}\right)U_{xi}, \qquad L_2(U_{\theta i}) = \left(\frac{\mathrm{d}^2}{\mathrm{d}\theta^2} + 1 + \frac{\rho\omega^2 R^2}{E}\right)\frac{\mathrm{d}U_{\theta i}}{\mathrm{d}\theta}.$$

Further, substituting Q_{xi} of equation (19a) and M_{zi} of equation (19f) into equation (20f) and employing Φ_{zi} of equation (21) into the result yields

$$L_3(U_{xi}) + L_4(U_{\theta i}) = 0, \tag{23}$$

where

$$L_3(U_{xi}) = \left\{\left(1 + \frac{\kappa_1 G}{E}\right)\frac{\mathrm{d}^2}{\mathrm{d}\theta^2} - \frac{\kappa_1 GAR^2}{EI_z} + \left(1 + \frac{\kappa_1 G}{E}\right)\frac{\rho\omega^2 R^2}{E}\right\}\frac{\mathrm{d}U_{xi}}{\mathrm{d}\theta},$$

$$L_4(U_{\theta i}) = \left\{\frac{\mathrm{d}^4}{\mathrm{d}\theta^4} + \left[\left(\frac{2\rho\omega^2 R^2 - \kappa_1 G}{E}\right) - \frac{\kappa_1 GAR^2}{EI_z}\right]\frac{\mathrm{d}^2}{\mathrm{d}\theta^2} + \frac{\rho\omega^2 R^2}{E}\left(\frac{\rho\omega^2 R^2 - \kappa_1 G}{E} - \frac{\kappa_1 GAR^2}{EI_z}\right)\right\}U_{\theta i}.$$

Combining equations (22) and (23) yields

$$\left(\frac{\mathrm{d}^6}{\mathrm{d}\theta^6} + c_1\frac{\mathrm{d}^4}{\mathrm{d}\theta^4} + c_2\frac{\mathrm{d}^2}{\mathrm{d}\theta^2} + c_3\right)(U_{\theta i}, U_{xi}) = (0, 0), \tag{24a, b}$$

where

$$c_1 = \frac{\rho\omega^2 R^2}{E}\left(2 + \frac{E}{\kappa_1 G}\right) + 2,$$

$$c_2 = \left(\frac{\rho\omega^2 R^2}{E}\right)^2\left(1 + \frac{2E}{\kappa_1 G}\right) + \frac{\rho\omega^2 R^2}{E}\left(1 - \frac{E}{\kappa_1 G} - \frac{AR^2}{I_z}\right) + 1,$$

$$c_3 = \left(\frac{\rho\omega^2 R^2}{E}\right)^3\frac{E}{\kappa_1 G} - \left(\frac{\rho\omega^2 R^2}{E}\right)^2\left(1 + \frac{E}{\kappa_1 G} + \frac{AR^2}{I_z}\right) + \frac{\rho\omega^2 R^2}{E}\left(1 + \frac{AR^2}{I_z}\right).$$

The frequency response of $U_{\theta i}$ is

$$U_{\theta i} = \sum_{j=1}^{6} a_{ji} g_j(\theta), \tag{25}$$

where $a_{1i} - a_{6i}$ are constants, the functions $g_1(\theta) \sim g_6(\theta)$ are listed in Appendix A. Substituting $U_{\theta i}$ of equation (25) into equation (22) and solving for U_{xi} yields

$$U_{xi} = \sum_{j=1}^{6} a_{ji} p_j(\theta), \tag{26}$$

where the functions $p_1(\theta) - p_6(\theta)$ are obtained by solving the differential equation

$$L_1(p_j) + L_2(g_j) = 0, \qquad j = 1\text{–}6. \tag{27}$$

Substituting U_{xi} of equation (26) and $U_{\theta i}$ of equation (25) into equation (21) yields

$$\Phi_{zi} = \sum_{j=1}^{6} a_{ji} p_j^*(\theta), \tag{28}$$

where

$$p_j^*(\theta) = \frac{\kappa_1 G + E}{\kappa_1 GR} \frac{\mathrm{d}p_j}{\mathrm{d}\theta} + \frac{1}{\kappa_1 GR}\left(\rho\omega^2 R^2 - \kappa_1 G + E\frac{\mathrm{d}^2}{\mathrm{d}\theta^2}\right) g_j.$$

Employing these values U_{xi} of equation (26), $U_{\theta i}$ of equation (25) and Φ_{zi} of equation (28) into equations (19a), (19b) and (19f) yields

$$(Q_{xi}, Q_{\theta i}, M_{zi})(\theta) = \sum_{j=1}^{6} a_{ji}(\eta_j, \beta_j, \zeta_j)(\theta), \tag{29}$$

where

$$\eta_j(\theta) = \frac{\kappa_1 GA}{R}\left(\frac{\mathrm{d}p_j}{\mathrm{d}\theta} - Rp_j^* - g_j\right), \qquad \beta_j(\theta) = \frac{EA}{R}\left(\frac{\mathrm{d}g_j}{\mathrm{d}\theta} + p_j\right), \qquad \zeta_j(\theta) = \frac{EI_z}{R}\frac{\mathrm{d}p_j^*}{\mathrm{d}\theta}.$$

The solutions for U_{zi}, Φ_{xi} and $\Phi_{\theta i}$ of the ith span to satisfy equations (20c)–(20e) are [9]

$$(U_z \;\; \Phi_x \;\; \Phi_\theta)_i(\theta) = \sum_{j=7}^{12} a_{ji}(g_j \;\; p_j \;\; p_j^*)(\theta), \tag{30}$$

where $a_{7i} - a_{12i}$ are constant, the functions $g_7(\theta) \sim g_{12}(\theta)$ are listed in Appendix B and

$$p_j(\theta) = \frac{1}{\kappa_1 GR}\left(\rho\omega^2 R^2 \int g_j \,\mathrm{d}\theta + \kappa_1 G \frac{\mathrm{d}g_j}{\mathrm{d}\theta}\right),$$

$$p_j^*(\theta) = \frac{1}{EI_x + C}\left[\kappa_1 GARg_j - (\kappa_1 GAR^2 + C - \rho\omega^2 R^2 I_x)\int p_j \,\mathrm{d}\theta + EI_x \frac{\mathrm{d}p_j}{\mathrm{d}\theta}\right]$$

for $j = 7$–12. The corresponding stress resultants and stress-couple resultants are

$$(Q_z, M_x, M_\theta)_i(\theta) = \sum_{j=7}^{12} a_{ji}(\eta_j, \beta_j, \zeta_j)(\theta), \tag{31}$$

where

$$\eta_j(\theta) = \kappa_1 GA\left(\frac{1}{R}\frac{\mathrm{d}g_j}{\mathrm{d}\theta} - p_j\right), \qquad \beta_j(\theta) = \frac{EI_x}{R}\left(p_j^* - \frac{\mathrm{d}p_j}{\mathrm{d}\theta}\right), \qquad \zeta_j(\theta) = \frac{C}{R}\left(p_j + \frac{\mathrm{d}p_j^*}{\mathrm{d}\theta}\right)$$

for $j = 7$–12.

Combining equations (25), (26) and (28)–(31) yields the frequency responses of the ith span into a vector form

$$\{U_{xi}\ U_{\theta i}\ U_{zi}\ \Phi_{xi}\ \Phi_{\theta i}\ \Phi_{zi}\ Q_{xi}\ Q_{\theta i}\ Q_{zi}\ M_{xi}\ M_{\theta i}\ M_{zi}\}^T(\theta) = [A_1(\theta)]\boldsymbol{\chi}_i, \tag{32}$$

where

$$\boldsymbol{\chi}_i = \{a_{1i}\ a_{2i}\ a_{3i}\ a_{4i}\ a_{5i}\ a_{6i}\ a_{7i}\ a_{8i}\ a_{9i}\ a_{10i}\ a_{11i}\ a_{12i}\}^T$$

Substituting equation (32) into equations (18a) and (18b) and then using the results in equations (11a)–(11d) yields the response vectors at two ends of the ith span as two symbolic forms

$$\begin{Bmatrix}\mathbf{D}_r\\ \mathbf{F}_r\end{Bmatrix} = [B_r]_i\chi_i, \qquad \begin{Bmatrix}\mathbf{D}_l\\ \mathbf{F}_l\end{Bmatrix}_i = [B_l]_i\chi_i, \tag{33a, b}$$

where the displacement vectors $\{\mathbf{D}_r\}_i$, $\{\mathbf{D}_l\}_i$, the force vectors $\{\mathbf{F}_r\}_i$ and $\{\mathbf{F}_l\}_i$ are

$$\{\mathbf{D}_r\}_i = \{U_{xi}\ U_{\theta i}\ U_{zi}\ \Phi_{xi}\ \Phi_{\theta i}\ -\Phi_{zi}\}^T(0), \tag{34a}$$

$$\{\mathbf{F}_r\}_i = \{-Q_{xi}\ -Q_{\theta i}\ -Q_{zi}\ M_{xi}\ -M_{\theta i}\ -M_{zi}\}^T(0), \tag{34b}$$

$$\{\mathbf{D}_l\}_i = \{U_{xi}\ U_{\theta i}\ U_{zi}\ \Phi_{xi}\ \Phi_{\theta i}\ -\Phi_{zi}\}^T(\alpha), \tag{34c}$$

$$\{\mathbf{F}_l\}_i = \{Q_{xi}\ Q_{\theta i}\ Q_{zi}\ -M_{xi}\ M_{\theta i}\ M_{zi}\}^T(\alpha). \tag{34d}$$

Solving the vector $\boldsymbol{\chi}_i$ from equation (33a) and substituting the result into equation (33b) yields the responses relation at both ends of the span as the form

$$\begin{Bmatrix}\mathbf{D}_l\\ \mathbf{F}_l\end{Bmatrix}_i = [C]_i\begin{Bmatrix}\mathbf{D}_r\\ \mathbf{F}_r\end{Bmatrix}_i, \tag{35}$$

where the matrix $[C]_i$ is

$$[C]_i = [B_l]_i[B_r]_i^{-1}.$$

3.2. COLUMN

The displacements, rotation angles and their corresponding stress resultants and stress-couple resultants of the column are expressed as

$$\{\overline{u_x}\ \overline{u_y}\ \overline{u_z}\ \overline{\phi_x}\ \overline{\phi_y}\ \overline{\phi_z}\}(z, t) = \{\overline{U_x}\ \overline{U_y}\ \overline{U_z}\ \overline{\Phi_x}\ \overline{\Phi_y}\ \overline{\Phi_z}\}(z)\sin(\omega t), \tag{36a}$$

$$\{\overline{q_x}\ \overline{q_y}\ \overline{q_z}\ \overline{m_x}\ \overline{m_y}\ \overline{m_z}\}(z, t) = \{\overline{Q_x}\ \overline{Q_y}\ \overline{Q_z}\ \overline{M_x}\ \overline{M_y}\ \overline{M_z}\}(z)\sin(\omega t), \tag{36b}$$

where

$$\overline{Q_x} = \kappa_2 GA^*\left(\frac{\mathrm{d}\overline{U_x}}{\mathrm{d}z} - \overline{\Phi_y}\right), \qquad \overline{Q_y} = \kappa_2 GA^*\left(\frac{\mathrm{d}\overline{U_y}}{\mathrm{d}z} - \overline{\Phi_x}\right), \qquad \overline{Q_z} = EA^*\frac{\mathrm{d}\overline{U_z}}{\mathrm{d}z}, \tag{37a, b, c}$$

$$\overline{M_x} = -EI^*\frac{\mathrm{d}\overline{\Phi_x}}{\mathrm{d}z}, \qquad \overline{M_z} = GJ^*\frac{\mathrm{d}\overline{\Phi_z}}{\mathrm{d}z}, \qquad \overline{M_y} = -EI^*\frac{\mathrm{d}\overline{\Phi_y}}{\mathrm{d}z}. \tag{37d, e, f}$$

Moreover, equations (14a)–(14f) become

$$-\frac{\mathrm{d}\overline{Q_x}}{\mathrm{d}z} = \rho A^* \omega^2 \overline{U_x}, \qquad -\frac{d\overline{Q_y}}{\mathrm{d}z} = \rho A^* \omega^2 \overline{U_y}, \qquad -\frac{d\overline{Q_z}}{\mathrm{d}z} = \rho A^* \omega^2 \overline{U_z}, \quad (38a, b, c)$$

$$-\overline{Q_y} + \frac{\mathrm{d}\overline{M_x}}{\mathrm{d}z} = \rho I^* \omega^2 \overline{\Phi_x}, \qquad -\overline{Q_x} + \frac{\mathrm{d}\overline{M_y}}{\mathrm{d}z} = \rho I^* \omega^2 \overline{\Phi_y}, \qquad -\frac{\mathrm{d}\overline{M_z}}{\mathrm{d}z} = \rho J^* \omega^2 \overline{\Phi_z}. \quad (38d, e, f)$$

Substituting $\overline{Q_x}$ of equation (37a) into equation (38a) and solving $\overline{\Phi_y}$ in terms of $\overline{U_x}$ yields

$$\frac{\mathrm{d}\overline{\Phi_y}}{\mathrm{d}z} = \frac{\mathrm{d}^2\overline{U_x}}{\mathrm{d}z^2} + \frac{\rho\omega^2}{\kappa_2 G}\overline{U_x}. \quad (39a)$$

Further, uncoupling equations (38a) and (38e) in terms of $\overline{U_x}$ or $\overline{\Phi_y}$ yields

$$\left\{\frac{\mathrm{d}^4}{\mathrm{d}z^4} + \frac{\rho\omega^2}{E}\left(1 + \frac{E}{\kappa_2 G}\right)\frac{\mathrm{d}^2}{\mathrm{d}z^2} + \frac{\rho\omega^2}{E}\left(\frac{\rho\omega^2}{\kappa_2 G} - \frac{A^*}{I^*}\right)\right\}(\overline{U_x}, \overline{\Phi_y}) = (0, 0), \quad (39b, c)$$

which are the equations of the Timoshenko beam. Similarly, the following three equations are obtained

$$\frac{\mathrm{d}\overline{\Phi_x}}{\mathrm{d}z} = \frac{\mathrm{d}^2\overline{U_y}}{\mathrm{d}z^2} + \frac{\rho\omega^2}{\kappa_2 G}\overline{U_y}, \quad (40a)$$

$$\left\{\frac{\mathrm{d}^4}{\mathrm{d}z^4} + \frac{\rho\omega^2}{E}\left(1 + \frac{E}{\kappa_2 G}\right)\frac{\mathrm{d}^2}{\mathrm{d}z^2} + \frac{\rho\omega^2}{E}\left(\frac{\rho\omega^2}{\kappa_2 G} - \frac{A^*}{I^*}\right)\right\}(\overline{U_y}, \overline{\Phi_x}) = (0, 0). \quad (40b, c)$$

The frequency responses of the column to satisfy the boundary conditions at the fixed end $z = 0$ are

$$\begin{aligned}
&\overline{U_x}(z) = b_3 f_3(z) + b_4 f_4(z), \quad \overline{U_y}(z) = b_5 f_3(z) + b_6 f_4(z), \quad \overline{U_z}(z) = b_1 f_1(z),\\
&\overline{\Phi_x}(z) = b_5 f_5(z) + b_6 f_6(z), \quad \overline{\Phi_y}(z) = b_3 f_5(z) + b_4 f_6(z), \quad \overline{\Phi_z}(z) = b_2 f_2(z),\\
&\overline{Q_x}(z) = b_3 f_9(z) + b_4 f_{10}(z), \quad \overline{Q_y}(z) = b_5 f_9(z) + b_6 f_{10}(z), \quad \overline{Q_z}(z) = b_1 f_7(z),\\
&\overline{M_x}(z) = b_5 f_{11}(z) + b_6 f_{12}(z), \quad \overline{M_y}(z) = b_3 f_{11}(z) + b_4 f_{12}(z), \quad \overline{M_z}(z) = b_2 f_8(z), \quad (41)
\end{aligned}$$

where b_1–b_6 denote constants and these functions are

$$f_1(z) = \sin\left(\sqrt{\frac{\rho}{E}}\,\omega z\right), \qquad f_2(z) = \sin\left(\sqrt{\frac{\rho}{G}}\,\omega z\right), \qquad f_7(z) = EA^*\frac{\mathrm{d}f_1}{\mathrm{d}z}, \qquad f_8(z) = GJ^*\frac{\mathrm{d}f_2}{\mathrm{d}z},$$

$$f_9(z) = \kappa_2 GA^*\left(\frac{\mathrm{d}f_3}{\mathrm{d}z} - f_5\right), \qquad f_{10}(z) = \kappa_2 GA^*\left(\frac{\mathrm{d}f_4}{\mathrm{d}z} - f_6\right), \qquad f_{11}(z) = -EI^*\frac{\mathrm{d}f_5}{\mathrm{d}z},$$

$$f_{12}(z) = -EI^*\frac{\mathrm{d}f_6}{\mathrm{d}z},$$

These functions f_3–f_6 are listed in Appendix C. Equation (41) constitutes the frequency responses of the column. Substituting equation (41) into equations (36a) and (36b) and then incorporating the results into equations (15a) and (15b) yields the response vectors at the top of the column as the symbolic forms

$$\{\overline{\mathbf{D}_l}\} = [G_1]\boldsymbol{\xi}, \qquad \{\overline{\mathbf{F}_l}\} = [G_2]\boldsymbol{\xi}, \quad (42a, b)$$

where $[G_1]$ and$[G_2]$ denote two matrices of order 6 by 6 and the constant vector $\boldsymbol{\xi}$, the displacement vector $\{\overline{\mathbf{D}_l}\}$ and the force vector $\{\overline{\mathbf{F}_l}\}$ are

$$\boldsymbol{\xi} = \{b_1 \;\; b_2 \;\; b_3 \;\; b_4 \;\; b_5 \;\; b_6\}^T, \tag{43}$$

$$\{\overline{\mathbf{D}_l}\} = \{\overline{U_x} \;\; \overline{U_y} \;\; \overline{U_z} \;\; \overline{\Phi_x} \;\; -\overline{\Phi_y} \;\; \overline{\Phi_z}\}^T(h), \tag{44a}$$

$$\{\overline{\mathbf{F}_l}\} = \{\overline{Q_x} \;\; \overline{Q_y} \;\; \overline{Q_z} \;\; \overline{M_x} \;\; -\overline{M_y} \;\; \overline{M_z}\}^T(h). \tag{44b}$$

3.3. ENTIRE STRUCTURE

The displacements continuity, forces balance and moments balance at the junction of two adjacent spans and the column of the frame (see Figure 3) are

$$\{\mathbf{D}_l\}_1 = \{\mathbf{D}_r\}_2 = \{\overline{\mathbf{D}_l}\}, \qquad \{\mathbf{F}_l\}_1 + \{\mathbf{F}_r\}_2 + \{\overline{F_l}\} = \{0 \;\; 0 \;\; 0 \;\; 0 \;\; 0 \;\; 0\}^T \tag{45a, b}$$

Substituting equation (45a) into equation (42a) and solving the constant vector $\boldsymbol{\xi}$ yields

$$\boldsymbol{\xi} = [G_1]^{-1}\{\mathbf{D}_l\}_1. \tag{46}$$

Equation (42b) will become the form

$$\{\overline{\mathbf{F}_l}\} = [G_2][G_1]^{-1}\{\mathbf{D}_l\}_1. \tag{47}$$

Substituting equation (47) into equation (45b) and combining the result with equation (45a) yields the following relation in the vector form

$$\begin{Bmatrix} \mathbf{D}_r \\ \mathbf{F}_r \end{Bmatrix}_2 = [Z]\begin{Bmatrix} \mathbf{D}_l \\ \mathbf{F}_l \end{Bmatrix}_1 \tag{48}$$

where

$$[Z] = \begin{bmatrix} I_{6\times 6} & O_{6\times 6} \\ -[G_2][G_1]^{-1} & -I_{6\times 6} \end{bmatrix},$$

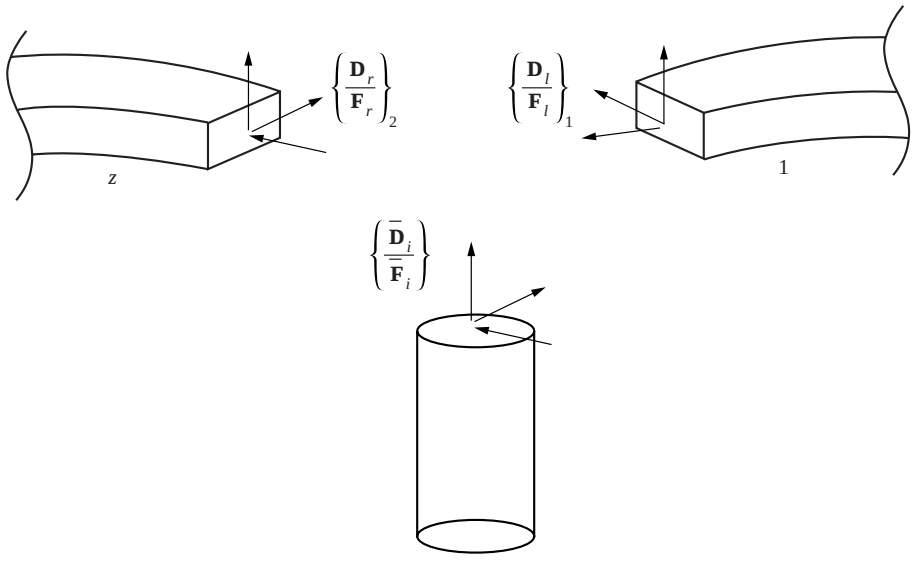

Figure 3. Applied end forces and displacements at the conjunction of two curved beams and one column.

where $I_{6\times 6}$ is an identity matrix and $O_{6\times 6}$ is a zero matrix. The responses relation at both ends of the entire curved beam is

$$\begin{Bmatrix}\mathbf{D}_l\\ \mathbf{F}_l\end{Bmatrix}_2 = \begin{bmatrix}T_{11} & T_{12}\\ T_{21} & T_{22}\end{bmatrix}\begin{Bmatrix}\mathbf{D}_r\\ \mathbf{F}_r\end{Bmatrix}_1, \tag{49}$$

where

$$\begin{bmatrix}T_{11} & T_{12}\\ T_{21} & T_{22}\end{bmatrix} = [C]_2[Z][C]_1.$$

The boundary conditions at both fixed ends imply

$$[T_{12}]\{\mathbf{F}_l\}_1 = \{0\ \ 0\ \ 0\ \ 0\ \ 0\ \ 0\}^T \tag{50}$$

to indicate that the ith modal frequency ω_i satisfies one eigenvalue of $[T_{12}]$ being zero. The corresponding set of displacements U_x^i, U_θ^i, U_z^i, rotation angles Φ_x^i, Φ_θ^i, Φ_z^i, stress resultants Q_x^i, Q_θ^i, Q_z^i and stress-couple resultants M_x^i, M_θ^i, M_z^i of the entire curved beam and those of $\overline{U_x^i}$, $\overline{U_y^i}$, $\overline{U_z^i}$, $\overline{\Phi_x^i}$, $\overline{\Phi_y^i}$, $\overline{\Phi_z^i}$, $\overline{Q_x^i}$, $\overline{Q_y^i}$, $\overline{Q_z^i}$, $\overline{M_x^i}$, $\overline{M_y^i}$, and $\overline{M_z^i}$ of the column can be obtained by doing similar calculations to those described by Wang and Lin [2].

4. ORTHOGONALITY

By performing similar procedures to those described by Wang and Lin [2], the following two equations are obtained:

$$\int_0^h \rho\{A^*(\overline{U_x^i}\,\overline{U_x^j} + \overline{U_y^i}\,\overline{U_y^j} + \overline{U_z^i}\,\overline{U_z^j}) + I^*(\overline{\Phi_x^i}\,\overline{\Phi_x^j} + \overline{\Phi_y^i}\,\overline{\Phi_y^j}) + J^*\overline{\Phi_z^i}\,\overline{\Phi_z^j}\}\,\mathrm{d}z$$

$$+\int_0^{2\alpha} \rho\{A(U_x^iU_x^j + U_\theta^iU_\theta^j + U_z^iU_z^j) + I_x\Phi_x^i\Phi_x^j + I_z\Phi_z^i\Phi_z^j + J\Phi_\theta^i\Phi_\theta^j\}R\,\mathrm{d}\theta = 0, \tag{51}$$

$$\int_0^{2\alpha}\left\{U_x^j\left(Q_\theta^i - \frac{\mathrm{d}Q_x^i}{\mathrm{d}\theta}\right) + U_\theta^j\left(-Q_x^i - \frac{\mathrm{d}Q_\theta^i}{\mathrm{d}\theta}\right) + U_z^j\left(-\frac{\mathrm{d}Q_z^i}{\mathrm{d}\theta}\right)\right\}\mathrm{d}\theta$$

$$+\int_0^{2\alpha}\left\{\Phi_x^j\left(-RQ_z^i + \frac{\mathrm{d}M_x^i}{\mathrm{d}\theta} + M_\theta^i\right) + \Phi_\theta^j\left(M_x^i - \frac{\mathrm{d}M_\theta^i}{\mathrm{d}\theta}\right) + \Phi_z^j\left(-RQ_x^i + \frac{\mathrm{d}M_z^i}{\mathrm{d}\theta}\right)\right\}\mathrm{d}\theta$$

$$+\int_0^h\left\{\overline{U_x^j}\left(-\frac{\mathrm{d}\overline{Q_x^i}}{\mathrm{d}z}\right) + \overline{U_y^j}\left(-\frac{\mathrm{d}\overline{Q_y^i}}{\mathrm{d}z}\right) + \overline{U_z^j}\left(-\frac{\mathrm{d}\overline{Q_z^i}}{\mathrm{d}z}\right)\right\}\mathrm{d}z$$

$$+\int_0^h\left\{\overline{\Phi_x^j}\left(\overline{Q_y^i} - \frac{\mathrm{d}\overline{M_x^i}}{\mathrm{d}z}\right) + \overline{\Phi_y^j}\left(-\overline{Q_x^i} + \frac{\mathrm{d}\overline{M_y^i}}{\mathrm{d}z}\right) + \overline{\Phi_z^j}\left(-\frac{\mathrm{d}\overline{M_z^i}}{\mathrm{d}z}\right)\right\}\mathrm{d}z = 0, \tag{52}$$

for $i \neq j$. Equations (51) and (52) indicate that the corresponding sets of mode shape functions of any two distinct modal frequencies are orthogonal to each other.

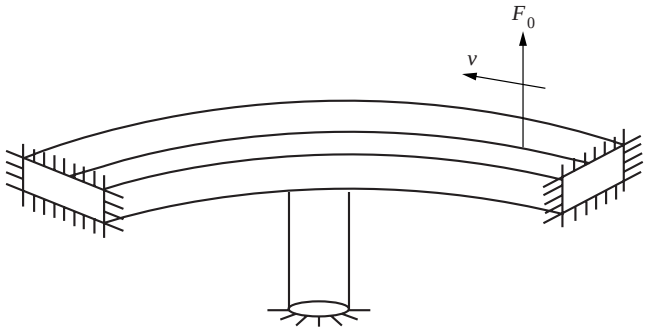

Figure 4. A concentrated load of magnitude F_0 traversing on the curved frame at a constant velocity v.

5. FORCED VIBRATION

While examining the forced vibration, the responses of the frame can be expressed by the mode superposition in the following forms:

$$(u_x\ u_\theta\ u_z\ \phi_x\ \phi_\theta\ \phi_z)(\theta, t) = \sum_{j=1} e_j(t)(U_x^j\ U_\theta^j\ U_z^j\ \Phi_x^j\ \Phi_\theta^j\ \Phi_z^j)(\theta), \tag{53a}$$

$$(q_x\ q_\theta\ q_z\ m_x\ m_\theta\ m_z)(\theta, t) = \sum_{j=1} e_j(t)(Q_x^j\ Q_\theta^j\ Q_z^j\ M_x^j\ M_\theta^j\ M_z^j)(\theta), \tag{53b}$$

for the curved beam and

$$(\overline{u_x}\ \overline{u_y}\ \overline{u_z}\ \overline{\phi_x}\ \overline{\phi_y}\ \overline{\phi_z})(z, t) = \sum_{j=1} e_j(t)(\overline{U_x^j}\ \overline{U_y^j}\ \overline{U_z^j}\ \overline{\Phi_x^j}\ \overline{\Phi_y^j}\ \overline{\Phi_z^j})(z), \tag{53c}$$

$$(\overline{q_x}\ \overline{q_y}\ \overline{q_z}\ \overline{m_x}\ \overline{m_y}\ \overline{m_z})(z, t) = \sum_{j=1} e_j(t)(\overline{Q_x^j}\ \overline{Q_y^j}\ \overline{Q_z^j}\ \overline{M_x^j}\ \overline{M_y^j}\ \overline{M_z^j})(z), \tag{53d}$$

for the column $e_j(t)$ is the jth modal amplitude of the frame. Performing similar procedures to those described by Wang and Lin [2] and employing the orthogonality of any two distinct sets of mode shape functions into the result yields

$$\Omega_i \frac{\mathrm{d}^2 e_i}{\mathrm{d}t^2} + \omega_i^2 \Omega_i e_i = W_i(t), \tag{54}$$

in which the ith modal mass Ω_i and excitation $W_i(t)$ are

$$\Omega_i = \int_0^{2\alpha} \rho\{A(U_x^{i^2} + U_\theta^{i^2} + U_z^{i^2}) + I_x\Phi_x^{i^2} + I_z\Phi_z^{i^2} + J\Phi_\theta^{i^2}\}R\,\mathrm{d}\theta$$

$$+ \int_0^h \rho\{A^*(\overline{U_x^{i^2}} + \overline{U_y^{i^2}} + \overline{U_z^{i^2}}) + I^*\overline{\Phi_x^{i^2}} + I^*\overline{\Phi_y^{i^2}} + J^*\overline{\Phi_z^{i^2}}\}\,\mathrm{d}z, \tag{55a}$$

$$W_i(t) = \int_0^{2\alpha} f(\theta, t)U_z^i(\theta)\,R\mathrm{d}\theta. \tag{55b}$$

TABLE 1

The effect of α on the comparison of the lowest three modal frequencies (rad/s) *of the curved frame* ($R = 150$ m, $r = 0{\cdot}5$ m, $a = 1$ m, $b = 0{\cdot}5$ m)

α (degrees)	ω_1	ω_2	ω_3
8	24·375	26·058	26·440
10	15·823	16·948	23·779
12	11·088	11·775	17·541

Equation (54) can be expressed as

$$\frac{d^2 e_i}{dt^2} + \omega_i^2 e_i = w_i(t), \tag{56}$$

in which the ith modal excitation per unit mass $w_i(t)$ is

$$w_i(t) = W_i(t)/\Omega_i. \tag{57}$$

A concentrated load of magnitude of F_0 moving at a constant velocity v on the curved beam of the frame is displayed in Figure 4. The form of the load is

$$f(\theta, t) = \begin{cases} F_0 \delta(\theta - vt/R) & 0 \leqslant t \leqslant 2T \\ 0 & 2T \leqslant t \end{cases}, \tag{58}$$

where δ is the impulse function and $T(= R\alpha/v)$ is the duration of load traversing on one span. The respective histories of the ith modal excitation per unit mass $w_i(t)$, amplitude $e_i(t)$ of the curved frame can be obtained by performing similar procedures to those described by Wang [11].

6. EXAMPLES AND DISCUSSION

In this section, the constants $E = 30$ GPa, $\rho = 2300$ kg/m^3, $\mu = 0{\cdot}2$, $\kappa_1 = 0{\cdot}833$, $a = 1\ m$, $b = 0{\cdot}5$ m, $\kappa_2 = 0{\cdot}878$, $r = 0{\cdot}5\ m$, $\kappa_3 = 0{\cdot}229$ and $R = 150$ m of the frame are considered. The magnitude of the moving force is $F_0 = 50$ kN. The initial conditions of the frame are set at zero. Both length and mass of the curved beam of the frame increase as α increases. Therefore, in Table 1 it is shown that the fundamental three modal frequencies of the frame ($h = 10$ m) decrease as α increases. A taller column causes the frame to have a heavier mass. Consequently, the longer a column is, the lower the modal frequencies of the frame ($\alpha = 10^\circ$) are, as indicated in Table 2. The lowest three modal frequencies and their corresponding mode shapes of the frame ($\alpha = 10^\circ$) are displayed in Figures 5(a)–(c).

TABLE 2

The effect of column height on the comparison of the lowest three modal frequencies (rad/s) *of the curved frame* ($\alpha = 10^\circ$, $R = 150$ m, $r = 0{\cdot}5$ m, $a = 1$ m, $b = 0{\cdot}5$ m)

h (m)	ω_1	ω_2	ω_3
8	15·991	16·950	25·319
10	15·823	16·948	23·779
12	15·658	16·945	21·702

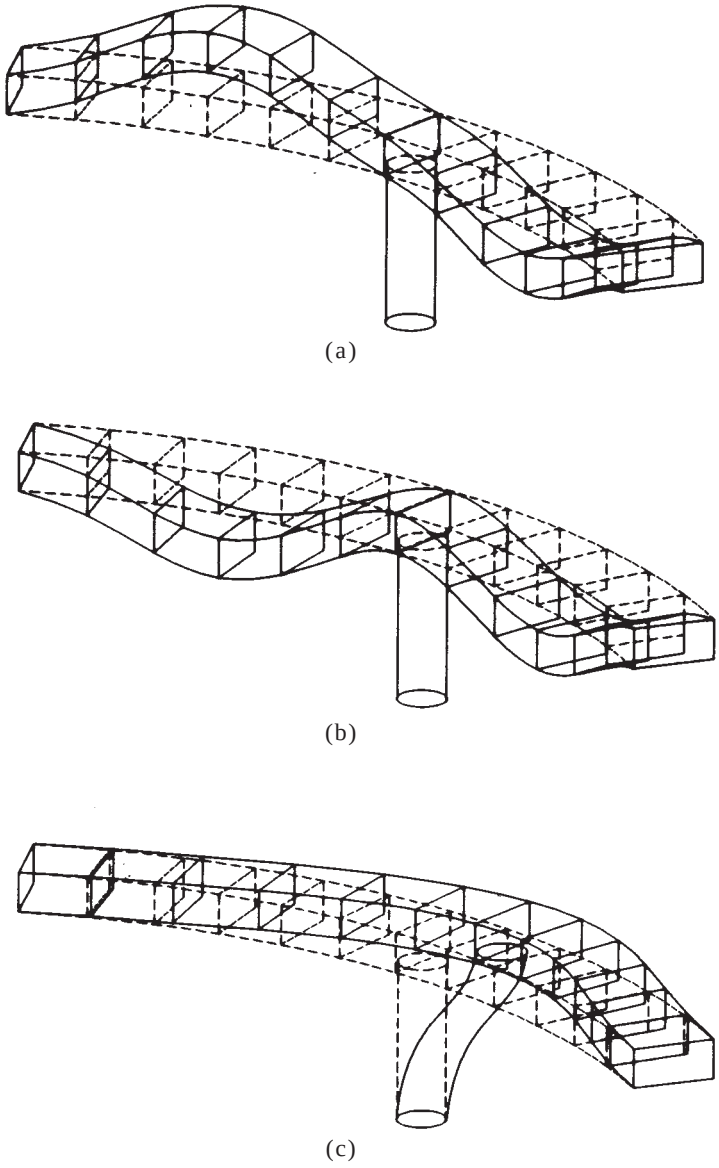

Figure 5. The lowest three modal frequencies and their corresponding mode shapes of the frame ($\alpha = 10^\circ$, $h = 10$ m): (a) the first mode, $\omega_1 = 15{\cdot}8232$ rad/s; (b) the second mode, $\omega_2 = 16{\cdot}9475$ rad/s; and (c) the third mode, $\omega_3 = 23{\cdot}7793$ rad/s.

Figures 5(a) and (b) illustrate the first and the second bending modes of the frame along the radial direction. Figure 5(c) depicts the bending mode of the frame along the z direction.

Results obtained by the method of modal analysis converge rather fast. The lowest three modes of the frame dominate the vibration of the structure. Therefore, it is sufficient to employ the lowest six modal frequencies and their corresponding sets of mode shape functions of the frame in the method of modal analysis in the numerical computation. The

velocity range considered in this section is 0 m/s $\leqslant v \leqslant$ 50 m/s. The following parameters are defined to illustrate the numerical results: strain energy for the cross-section of the mid-span of the first beam during the motion of force, $\overline{S}_b$ (J/m); strain energy for the cross-section of the mid-span of the column during the motion of force, $\overline{S}_c$ (J/m); strain energy of the entire beam during the motion of force, S_b (J); strain energy of the column during the motion of force, S_c (J); strain energy of the frame during the motion of force, S(J); maximum strain energy of the cross-section of the entire beam during the motion of force, $\overline{S}_{bmax}$ (J/m); maximum strain energy of the cross-section of the column during the motion of force, $\overline{S}_{cmax}$ (J/m); maximum strain energy of the entire beam during the motion of force, S_{bmax} (J); maximum strain energy of the column during the motion of force, S_{cmax} (J); maximum strain energy of the frame during the motion of force, S_{max} (J).

The comparisons of two different v effects on both histories of $\overline{S}_b$ and $\overline{S}_c$ of the frame ($\alpha = 10^\circ$, $h = 10$ m) are displayed in Figures 6(a) and (b), respectively. In Figure 6(a) it is shown that the peak of $\overline{S}_b$ always occurs while the force is crossing the mid-point of the first span. The results in Figure 6(b) reveal that two peaks of $\overline{S}_c$ always occur while the force crosses the mid-point of either the first span or the second span of the frame. Moreover, the magnitude of the second peak exceeds that of the first. A rapidly moving force can excite more modes of the frame than a slowly moving force can. Consequently, both $\overline{S}_b$ and $\overline{S}_c$ caused by a rapidly moving force exceed those by a slowly moving force.

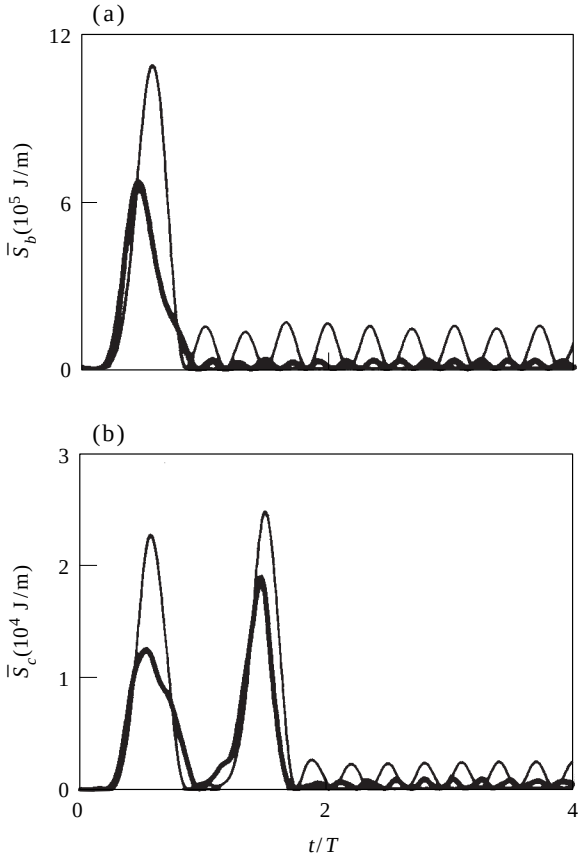

Figure 6. Comparison of two v effects of the moving load on: (a) $\overline{S}_b$ history and (b) $\overline{S}_c$ history of the frame ($\alpha = 10^\circ$, $h = 10$ m). ——, $v = 30$ m/s; ——, $v = 40$ m/s.

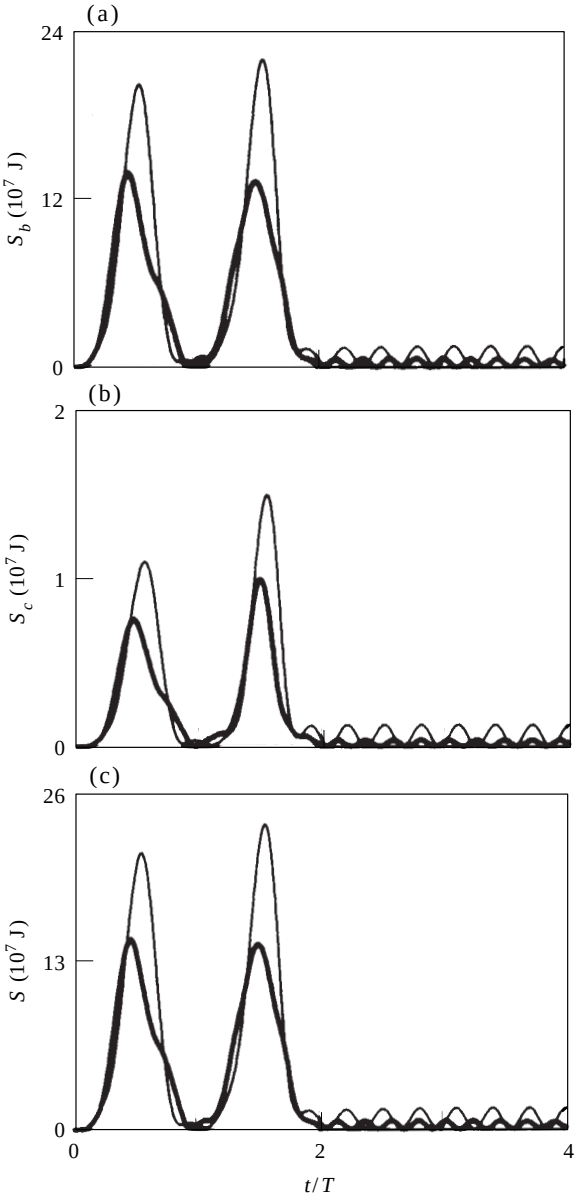

Figure 7. Comparisons of two v effects of the moving load on: (a) S_b history and (b) S_c history and (c) S history of the frame ($\alpha = 10^\circ$, $h = 10$ m). ——, $v = 30$ m/s; ——, $v = 40$ m/s.

The frame is in the state of free vibration after the force has left the structure. Therefore, both $\overline{S}_b$ and $\overline{S}_c$ are in a steady state of oscillation after the force has left the frame.

The comparisons of two different v effects on (a) the S_b history, (b) the S_c history and (c) the S history of the frame ($\alpha = 10^\circ$, $h = 10$ m) are displayed in Figures 7(a)–(c), respectively. These results point to two peaks in each figure. Furthermore, these peaks always occur while the force is crossing the mid-span of either the first span or the second span of the frame. Moreover, the results in each figure also reveal that the magnitude of

the second peak exceeds that of the first peak. A faster moving force induces the larger S_b, S_c and S of the frame.

The comparisons of two different h effects on the $\overline{S}_{bmax} - v$ distribution and the $\overline{S}_{cmax} - v$ distribution of the frame ($\alpha = 10^\circ$) are displayed in Figures 8(a) and (b), respectively. A short column causes a small deflection of the frame. Consequently, in Figure 8(b) it is indicated that a short column has a small $\overline{S}_{cmax}$. A short column causes large reaction forces and moments on the curved beam. Consequently, a short column causes the entire beam to have a large $\overline{S}_{bmax}$. All ends of the frame are fixed. Therefore, $\overline{S}_{bmax}$ usually appears near one fixed end of the curved beam. Moreover, $\overline{S}_{cmax}$ always occurs near the bottom of the column.

The comparisons of two different h effects on the $S_{bmax} - v$ distribution, the $S_{c,max} - v$ distribution and the S_{max}–V distribution of the frame ($\alpha = 10^\circ$) are displayed in Figures 9(a)–(c), respectively. In Figures 9(a)–(c) it is indicated that S_{bmax}, and S_{cmax} and S_{max} of the frame increase as the velocity of the force increases. Further, in Figure 9(b) it is also indicated that a short column has a small S_{cmax}. The length of one span beam exceeds that of the column. Therefore, two different column heights do not produce any significant deviation on these $S_{bmax} - v$ distributions and these $S_{max} - v$ distributions, as indicated in Figures 9(a) and (c).

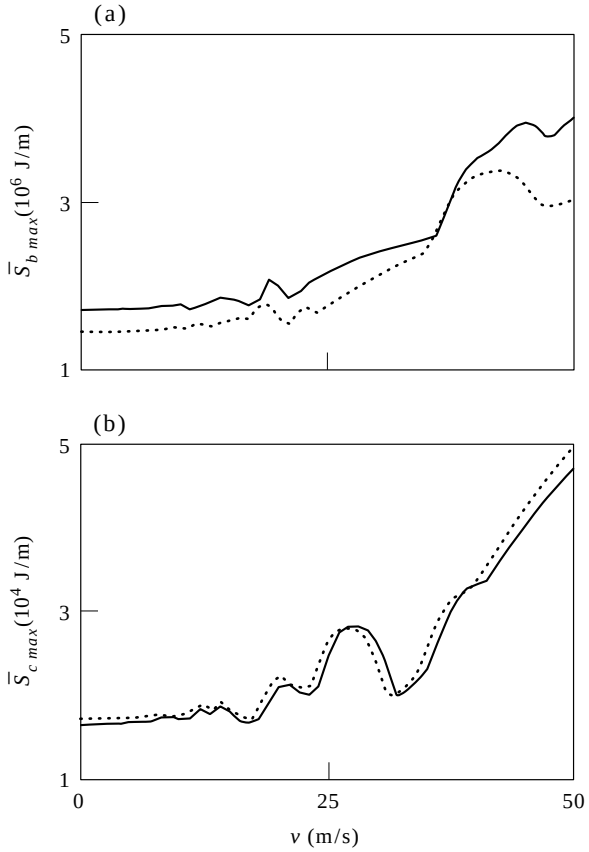

Figure 8. Comparisons of two h effects of the column on: (a) $\overline{S}_{bmax}$–v and (b) $\overline{S}_{cmax}$–v distributions of the frame ($\alpha = 10^\circ$). ——, $h = 8$ m; ——, $h = 12$ m.

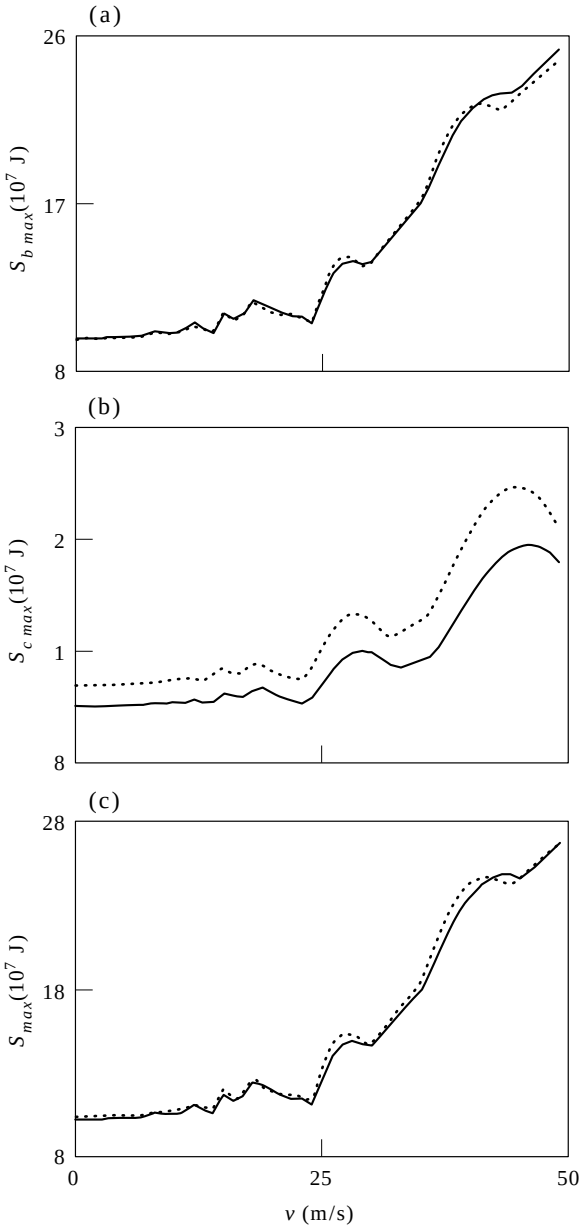

Figure 9. Comparisons of two h effects of the column on (a) S_{bmax}–v (b) S_{cmax}–v and (c) S_{max}–v distributions of the frame ($\alpha = 10^\circ$). ——, $h = 8$ m; · · · · ·, $h = 12$ m.

7. CONCLUSIONS

This study formulates the equations of motion of a T-type curved frame. The first mode of the frame is a bending mode. The problems of a moving load on the curved frame are also examined analytically. A taller column of the frame causes less maximum strain energy per unit length in the curved beam; however, more maximum strain energy occurs in the column. The maximum strain energy per unit length always appears near one fixed end of the frame.

ACKNOWLEDGMENT

This work was sponsored by the National Science Council, Republic of China, under Contract No. 87-2212-E006-035. The financial support is greatly acknowledged.

REFERENCES

1. R. T. WANG and J. L. JENG 1996 *Journal of the Chinese Institute of Engineers* **19**, 409–416. Dynamic analysis of a T-type Timoshenko frame to a moving load using finite element method.
2. R. T. WANG and J. S. LIN 1998 *Journal of Sound and Vibration* **212**, 417–434. Vibration of multi-span Timoshenko frames due to moving loads.
3. E. VOLTERRA and J. H. GAINES 1971 *Advanced Strength of Materials*. Englewood Cliffs, NJ: Prentice-Hall.
4. F. M. EL-AMIN and M. A. KASEM 1978 *International Journal for Numerical Methods in Engineering* **12**, 159–167. Higher-order horizontally-curved beam finite element including warping for steel bridges.
5. A. O. LEBECK and J. S. KNOWLTON 1985 *International Journal for Numerical Methods in Engineering* **21**, 421–435. A finite element for the three-dimensional deformation of a circular ring.
6. S. S. RAO 1971 *Journal of Sound and Vibration* **16**, 551–566. Effects of transverse shear and rotatory inertia on the coupled twist-bending vibrations of circular rings.
7. T. M. WANG, A. J. LASKEY and M. F. AHMAD 1984 *International Journal of Solids and Structures* **20**, 257–265. Natural frequencies for out-of-plane vibrations of continuous curved beams considering shear and rotatory inertia.
8. J. M. M. SILVA and A. P. V. URGUEIRA 1988 *International Journal of Solids and Structures* **24**, 271–284. Out-of-plane dynamic response of curved beams—an analytical model.
9. R. T. WANG and Y. L. SANG 1998 *Structural Engineering and Mechanics*, *An International Journal* (accepted). Out-of-plane vibration of multi-span curved beam due to moving loads.
10. S. P. TIMOSHENKO and J. N. GOODIER 1970 *Theory of Elasticity*. New York: McGraw-Hill.
11. R. T. WANG 1997 *Journal of Sound and Vibration* **207**, 731–742. Vibration of multi-span Timoshenko beams to a moving force.

APPENDIX A: LIST OF FUNCTIONS $g_1(\theta) \sim g_6(\theta)$

These functions $g_1(\theta) \sim g_6(\theta)$ depend on the roots $\lambda_i (i = 1, 2, 3)$ of the equation

$$\lambda_i^6 + c_1\lambda_i^4 + c_2\lambda_i^2 + c_3 = 0. \tag{A1}$$

There are six kinds of $g_1(\theta) \sim g_6(\theta)$

(1) For $\lambda_1 < \lambda_2 < \lambda_3 < 0$

$$\{g_1(\theta)\ g_2(\theta)\ g_3(\theta)\ g_4(\theta)\ g_5(\theta)\ g_6(\theta)\} = \{\cos(\alpha_1\theta)\sin(\alpha_1\theta)\ \cos(\alpha_2\theta)\sin(\alpha_2\theta)\ \cos(\alpha_3\theta)\sin(\alpha_3\theta)\}, \tag{A2}$$

where $\alpha_i = \sqrt{|\lambda_i|}$, $i \sim 3$.

(2) For $\lambda_1 < \lambda_2 < 0 < \lambda_3$

$$\{g_1(\theta)\ g_2(\theta)\ g_3(\theta)\ g_4(\theta)\ g_5(\theta)\ g_6(\theta)\} = \{\cos(\alpha_1\theta)\sin(\alpha_1\theta)\ \cos(\alpha_2\theta)\sin(\alpha_2\theta)\ \cosh(\alpha_3\theta)\sinh(\alpha_3\theta)\}. \tag{A3}$$

(3) For $\lambda_1 < 0 < \lambda_2 < \lambda_3$

$$\{g_1(\theta)\ g_2(\theta)\ g_3(\theta)\ g_4(\theta)\ g_5(\theta)\ g_6(\theta)\} = \{\cos(\alpha_1\theta)\sin(\alpha_1\theta)\ \cosh(\alpha_2\theta)\sinh(\alpha_2\theta)\ \cosh(\alpha_3\theta)\sinh(\alpha_3\theta)\}, \tag{A4}$$

where $\alpha_i = \sqrt{|\lambda_i|}$, $i = 1 \sim 3$.

(4) For $0 < \lambda_2 < \lambda_3 < \lambda_1$

$$\{g_1(\theta)\ g_2(\theta)\ g_3(\theta)\ g_4(\theta)\ g_5(\theta)\ g_6(\theta)\} = \{\cosh(\alpha_1\theta)\sinh(\alpha_1\theta)\ \cosh(\alpha_2\theta)\sinh(\alpha_2\theta)\ \cosh(\alpha_3\theta)\sinh(\alpha_3\theta)\}. \quad \text{(A5)}$$

(5) For $\lambda_1 < 0$, two conjugate λ_2 and $\overline{\lambda_2}$

$$\{g_1(\theta)\ g_2(\theta)\ g_3(\theta)\ g_4(\theta)\ g_5(\theta)\ g_6(\theta)\} = \{\cos(\alpha_1\theta)\sin(\alpha_1\theta)\ \cos(\sigma\theta)\cosh(\chi\theta)\ \cos(\sigma\theta)\sinh(\chi\theta)\ \sin(\sigma\theta)\cosh(\chi\theta)\sin(\sigma\theta)\sinh(\chi\theta)\}, \quad \text{(A6)}$$

where $\sigma = |\lambda_2|^{1/2}\cos(0{\cdot}5\arg(\lambda_2))$ and $\chi = \pm|\lambda_2|^{1/2}\sin(0{\cdot}5\arg(\lambda_2))$.

(6) For $\lambda_1 > 0$, two conjugate λ_2 and $\overline{\lambda_2}$

$$\{g_1(\theta)\ g_2(\theta)\ g_3(\theta)\ g_4(\theta)\ g_5(\theta)\ g_6(\theta)\} = \{\cosh(\alpha_1\theta)\sinh(\alpha_1\theta)\ \cos(\sigma\theta)\cosh(\chi\theta)\ \cos(\sigma\theta)\sinh(\chi\theta)\ \sin(\sigma\theta)\cosh(\chi\theta)\sin(\sigma\theta)\sinh(\chi\theta)\}. \quad \text{(A7)}$$

APPENDIX B: LIST OF THE FUNCTIONS $g_7(\theta) \sim g_{12}(\theta)$

These functions $g_7(\theta) \sim g_{12}(\theta)$ depend on the roots $\lambda_i (i = 1, 2, 3)$ of the equation

$$\lambda_i^6 + c_4\lambda_i^4 + c_5\lambda_i^2 + c_6 = 0, \quad \text{(B1)}$$

where

$$c_4 = 2 + \rho R^2\omega^2\left(\frac{J}{C} + \frac{1}{E} + \frac{1}{\kappa_1 G}\right),$$

$$c_5 = 1 - \rho R^2\omega^2\left(\frac{I}{C} + \frac{J}{EI} - \frac{2}{\kappa_1 G} + \frac{AR^2}{EI}\right) + \rho^2 R^2\omega^4\left(\frac{J}{\kappa_1 GC} + \frac{J}{CE} + \frac{1}{\kappa_1 GE}\right),$$

$$c_6 = \rho R^2\omega^2\left(\frac{I}{\kappa_1 G} + \frac{AR^2}{C}\right) - \rho^2 R^4\omega^4\left(\frac{I}{\kappa_1 GC} + \frac{J}{\kappa_1 GEI} + \frac{AR^2 J}{CEI}\right) + \frac{\rho^3 R^6\omega^6 J}{\kappa_1 GEC}$$

There are six kinds of $g_7(\theta) \sim g_{12}(\theta)$:

(1) For $\lambda_1 < \lambda_2 < \lambda_3 < 0$

$$\{g_7(\theta)\ g_9(\theta)\ g_9(\theta)\ g_{10}(\theta)\ g_{11}(\theta)\ g_{12}(\theta)\} = \{\cos(\alpha_1\theta)\sin(\alpha_1\theta)\ \cos(\alpha_2\theta)\sin(\alpha_2\theta)\ \cos(\alpha_3\theta)\sin(\alpha_3\theta)\}, \quad \text{(B2)}$$

where $\alpha_i = \sqrt{|\lambda_i|}$, $i = 1 \sim 3$.

(2) For $\lambda_1 < \lambda_2 < 0 < \lambda_3$

$$\{g_7(\theta)\ g_8(\theta)\ g_9(\theta)\ g_{10}(\theta)\ g_{11}(\theta)\ g_{12}(\theta)\} = \{\cos(\alpha_1\theta)\sin(\alpha_1\theta)\ \cos(\alpha_2\theta)\sin(\alpha_2\theta)\ \cosh(\alpha_3\theta)\sinh(\alpha_3\theta)\}. \quad \text{(B3)}$$

(3) For $\lambda_1 < 0 < \lambda_2 < \lambda_3$

$$\{g_7(\theta)\ g_8(\theta)\ g_9(\theta)\ g_{10}(\theta)\ g_{11}(\theta)\ g_{12}(\theta)\} = \{\cos(\alpha_1\theta)\sin(\alpha_1\theta)\ \cosh(\alpha_2\theta)\sinh(\alpha_2\theta)\ \cosh(\alpha_3\theta)\sinh(\alpha_3\theta)\}, \quad \text{(B4)}$$

where $\alpha_i = \sqrt{|\lambda_i|}$, $i = 1 \sim 3$.

(4) For $0 < \lambda_2 < \lambda_3 < \lambda_1$

$$\{g_7(\theta)\ g_8(\theta)\ g_9(\theta)\ g_{10}(\theta)\ g_{11}(\theta)\ g_{12}(\theta)\} = \{\cosh(\alpha_1\theta)\sinh(\alpha_1\theta)\ \cosh(\alpha_2\theta)\sinh(\alpha_2\theta)\ \cosh(\alpha_3\theta)\sinh(\alpha_3\theta)\}. \quad \text{(B5)}$$

(5) For $\lambda_1 < 0$, two conjugate λ_2 and $\overline{\lambda_2}$

$$\{g_7(\theta)\ g_8(\theta)\ g_9(\theta)\ g_{10}(\theta)\ g_{11}(\theta)\ g_{12}(\theta)\} = \{\cos(\alpha_1\theta)\sin(\alpha_1\theta)\ \cos(\sigma\theta)\cosh(\chi\theta)\ \cos(\sigma\theta)\sinh(\chi\theta)\ \sin(\sigma\theta)\cosh(\chi\theta)\sin(\sigma\theta)\sinh(\chi\theta)\}, \quad \text{(B6)}$$

where $\sigma = |\lambda_2|^{1/2}\cos(0{\cdot}5\arg(\lambda_2))$ and $\chi = |\lambda_2|^{1/2}\sin(0{\cdot}5\arg(\lambda_2))$.

(6) For $\lambda_1 > 0$, two conjugate λ_2 and $\overline{\lambda_2}$

$$\{g_7(\theta)\ g_8(\theta)\ g_9(\theta)\ g_{10}(\theta)\ g_{11}(\theta)\ g_{12}(\theta)\} = \{\cosh(\alpha_1\theta)\sinh(\alpha_1\theta)\ \cos(\sigma\theta)\cosh(\chi\theta)\ \cos(\sigma\theta)\sinh(\chi\theta)\ \sin(\sigma\theta)\cosh(\chi\theta)\sin(\sigma\theta)\sinh(\chi\theta)\}. \quad \text{(B7)}$$

APPENDIX C: LIST OF FUNCTIONS $f_3(z) \sim f_6(z)$

(1) For $\rho\omega^2/\kappa_2 G < A^*/I^*$

$$f_3(z) = \sinh(\lambda_1 z) + \frac{r_1}{r_2}\sin(\lambda_2 z), \qquad f_4(z) = \cosh(\lambda_1 z) - \cos s(\lambda_2 z), \quad \text{(C1, 2)}$$

$$f_5(z) = r_1(\cosh(\lambda_1 z) - \cos s(\lambda_2 z)), \qquad f_6(z) = r_1\sinh(\lambda_1 z) - r_2\sin(\lambda_2 z), \quad \text{(C3, 4)}$$

where

$$\lambda_1^2 = -\frac{\rho\omega^2}{2E}\left(1 + \frac{E}{\kappa_2 G}\right) + \frac{1}{2}\sqrt{\left(\frac{\rho\omega^2}{E}\right)^2\left(1 - \frac{E}{\kappa_2 G}\right)^2 + \frac{4\rho\omega^2 A^*}{EI^*}},$$

$$\lambda_2^2 = \frac{\rho\omega^2}{2E}\left(1 + \frac{E}{\kappa_2 G}\right) + \frac{1}{2}\sqrt{\left(\frac{\rho\omega^2}{E}\right)^2\left(1 - \frac{E}{\kappa_2 G}\right)^2 + \frac{4\rho\omega^2 A^*}{EI^*}},$$

$$r_1 = \lambda_1 + \frac{\rho\omega^2}{\lambda_1\kappa_2 G}, \qquad r_2 = -\lambda_2 + \frac{\rho\omega^2}{\lambda_2\kappa_2 G}.$$

(2) For $\rho\omega^2/\kappa_2 G > A^*/I^*$

$$f_3(z) = \sin(\lambda_1 z) - \frac{s_1}{s_2}\sin(\lambda_2 z), \qquad f_4(z) = \cos(\lambda_1 z) - \cos s(\lambda_2 z), \quad \text{(C5, 6)}$$

$$f_5(z) = s_1(\cos(\lambda_1 z) - \cos s(\lambda_2 z)), \qquad f_6(z) = -s_1\sinh(\lambda_1 z) + s_2\sin(\lambda_2 z), \quad \text{(C7, 8)}$$

where

$$\lambda_1^2 = \frac{\rho\omega^2}{2E}\left(1 + \frac{E}{\kappa_2 G}\right) - \frac{1}{2}\sqrt{\left(\frac{\rho\omega^2}{E}\right)^2\left(1 - \frac{E}{\kappa_2 G}\right)^2 + \frac{4\rho\omega^2 A^*}{EI^*}},$$

$$\lambda_2^2 = \frac{\rho\omega^2}{2E}\left(1 + \frac{E}{\kappa_2 G}\right) + \frac{1}{2}\sqrt{\left(\frac{\rho\omega^2}{E}\right)^2\left(1 - \frac{E}{\kappa_2 G}\right)^2 + \frac{4\rho\omega^2 A^*}{EI^*}},$$

$$s_1 = \lambda_1 - \frac{\rho\omega^2}{\lambda_1\kappa_2 G}, \qquad s_2 = \lambda_2 - \frac{\rho\omega^2}{\lambda_2\kappa_2 G}.$$